JOURNAL OF Materials CHEMISTRY

Synthesis and characterisation of MCM-41-supported dimolybdenum complexes

Paula Ferreira,[a] Isabel S. Gonçalves,[a] Fritz E. Kühn,[b] Martyn Pillinger,[a] João Rocha,*[a] Alan Thursfield,[b] Wen-Mei Xue[b] and Guofang Zhang[b]

[a]*Department of Chemistry, University of Aveiro, 3810-193 Aveiro, Portugal. E-mail: rocha@dq.ua.pt; Fax: +351 34 370 084; Tel: +351 34 370 730*
[b]*Anorganisch-chemisches Institut der Technischen Universität München, Lichtenbergstraße 4, D-85747 Garching bei München, Germany*

Received 15th October 1999, Accepted 23rd March 2000
Published on the Web 4th May 2000

Isolated quadruply bonded dimolybdenum(II,II) complexes have been grafted onto the surface of hexagonal MCM-41 mesoporous silica by diffusion of an excess of the complex salts $[Mo_2(MeCN)_{10}][BF_4]_4$, $[Mo_2(\mu\text{-}O_2CMe)_2(MeCN)_6][BF_4]_2$ and $[Mo_2(\mu\text{-}O_2CMe)_2(dppa)_2(MeCN)_2][BF_4]_2$ into calcined and dehydrated MCM-41 in dry acetonitrile at room temperature. The physical properties of the resulting unstable materials, together with the nature of the host–guest interactions and the structure of supported molybdenum species, have been characterised by means of elemental analysis, powder X-ray diffraction, N_2 adsorption, FTIR and MAS NMR (^{13}C, ^{29}Si, ^{31}P) spectroscopy.

Introduction

Complexes containing the quadruply bonded dimolybdenum(II,II) $[Mo–Mo]^{4+}$ core are precursors to effective catalysts for a number of different organic transformations.[1] McCann and co-workers showed that complexes carrying labile nitrile ligands are efficient homogeneous and supported or unsupported heterogeneous catalysts for the ring-opening metathesis polymerisation of norbornene,[2] the polymerisation of cyclopentadiene and dicyclopentadiene,[3] and the polymerisation of phenylacetylene.[1] These studies were limited to *cis*-$[Mo_2(\mu\text{-}O_2CMe)_2(MeCN)_6][BF_4]_2$, $[Mo_2(MeCN)_{10}][BF_4]_4$, and their SiO_2-fixed derivatives. A very recent investigation shows that a broader variety of dimolybdenum complexes exhibit excellent activity as initiators in cationic polymerisation reactions.[4]

The initial anchoring of the $[Mo–Mo]^{4+}$ complexes to SiO_2 was thought to occur at the surface silanol (≡Si–OH) groups on removal of labile MeCN ligands from the complexes. However, these materials were not well characterised and there was no direct physical evidence for the exact nature of the final molybdenum species on the surface, that is, whether the Mo–Mo bond was retained (as observed for $[Mo_2(\mu\text{-}O_2CMe)_4]$–$SiO_2$[5]) or broken to give mononuclear species (as reported for $[Mo_2(C_3H_5)_4]$–SiO_2[6]).

There is now considerable interest in the application of the new generation of mesoporous siliceous and nonsiliceous oxides as catalyst support materials.[7] MCM-41 is one member of this family.[8] A generally accepted structural model for MCM-41 materials consists of a hexagonal arrangement of cylindrical pores embedded in a matrix of amorphous silica. The pore diameters are tuneable in the range 20–100 Å and the best materials have high surface areas (1000 $m^2\ g^{-1}$), high pore volumes (1 $cm^3\ g^{-1}$) and very narrow pore size distributions. They therefore have properties intermediate between those of amorphous refractory oxides and microporous crystalline molecular sieves. Like the commonly used silica and alumina supports, the inner surfaces of MCM-41 are covered with nucleophilic silanol groups which enable the immobilisation of transition metal catalysts by direct grafting with organometallic and transition metal complexes.

In this article we present a study of the heterogenisation of the dimolybdenum complexes $[Mo_2(MeCN)_{10}][BF_4]_4$, $[Mo_2(\mu\text{-}O_2CMe)_2(MeCN)_6][BF_4]_2$ and $[Mo_2(\mu\text{-}O_2CMe)_2(dppa)_2(MeCN)_2][BF_4]_2$ on the surface of purely siliceous MCM-41. The supported materials have been characterised by elemental analysis, powder X-ray diffraction (XRD), N_2 adsorption studies, FTIR and solid-state magic angle spinning (MAS) NMR (^{13}C, ^{29}Si, ^{31}P) spectroscopy.

Experimental

General

All preparations and manipulations were performed using standard Schlenk techniques under an oxygen-free and water-free nitrogen atmosphere. Commercial grade solvents were dried and deoxygenated by refluxing for at least 24 h over appropriate drying agents under nitrogen atmosphere and freshly distilled prior to use.

Powder X-ray diffraction data were collected on a Philips X'pert diffractometer using Cu-Kα radiation filtered by Ni ($\lambda = 1.5418$ Å). Microanalyses were performed at the TU Munich. Infrared spectra were recorded on a Unican Mattson Mod 7000 FTIR spectrophotometer using KBr pellets and/or solutions. ^{29}Si and ^{13}C NMR spectra were recorded at 79.49 and 100.62 MHz respectively, on a (9.4 T) Bruker MSL 400P spectrometer. ^{29}Si MAS NMR spectra were recorded with 40° pulses, spinning rates of 5.0–5.5 kHz and 60 s recycle delays. ^{29}Si CP MAS NMR spectra were recorded with 5.5 μs pulses, a spinning rate of 5.0 kHz and 4 s recycle delays. ^{13}C CP MAS NMR spectra were recorded with 4.5 μs pulses, a spinning rate of 8 kHz and 4 s recycle delays. Chemical shifts are quoted in parts per million from TMS. ^{31}P MAS NMR spectra were recorded at 162 MHz, using 45° pulses with recycle delays of 60 s and a spinning rate of 14 kHz. Chemical shifts are quoted in parts per million from H_3PO_4 (85%).

Nitrogen adsorption isotherms were recorded using a CI electronics MK2-M5 microbalance connected to a vacuum manifold line. The pristine MCM-41 starting material was dehydrated overnight at 723 K to an ultimate pressure of 10^{-4} mbar and then cooled to room temperature prior to adsorption. Extra care with the functionalised materials was necessary due to the possibility of aerial oxidation, therefore transfer to the balance and outgassing of the system was rapid.

A lower dehydration temperature (413 K) was used with these samples to further minimise destruction of the functionalities. Nitrogen isotherms were then recorded at 77 K. Equilibration of each data point was monitored using CI electronics' Labweigh software and the pressure monitored using an Edwards Barocel pressure sensor. Specific surface areas were determined from the linear part of the BET plot ($P/P_o = 0.05$–0.3).

$[Mo_2(MeCN)_{10}][BF_4]_4$ was prepared according to the literature procedure.[9] ^{13}C CP MAS NMR (25 °C): δ (ppm) = 149.5, 148.1 (Me**C**N, equatorial), 123.6 (Me**C**N, axial), 3.5, 0.8 (**Me**CN; equatorial and axial).

$[Mo_2(\mu\text{-}O_2CMe)_2(MeCN)_6][BF_4]_2$ was prepared according to the literature procedure.[10,11] ^{13}C CP MAS NMR (25 °C): δ (ppm) = 187.6 (**O$_2$C**Me), 148.9, 146.5 (Me**C**N), 121.9, 119.7, 118.3 (Me**C**N), 22.68 (O$_2$C**Me**), 5.0, 2.1, −0.1 (**Me**CN).

$[Mo_2(\mu\text{-}O_2CMe)_2(dppa)_2(MeCN)_2][BF_4]_2$ was prepared according to the literature procedure.[11] ^{13}C CP MAS NMR (25 °C): δ (ppm) = 189.3 (s, **O$_2$C**Me), 134.2, 131.1, 129.5 (dppa), 24.6, 22.4 (s, O$_2$C**Me**), 1.9, 0.1 (**Me**CN). ^{31}P MAS NMR spectrum (25 °C): δ (ppm) = 82.6.

Purely siliceous MCM-41 was synthesised as described previously using $[(C_{14}H_{29})NMe_3]Br$ as the templating agent.[8] After calcination (540 °C/6 h), the material was characterised by XRD, N_2 adsorption and IR spectroscopy. Prior to the grafting experiments, calcined MCM-41 was activated at 160 °C *in vacuo* (10^{-2} Pa) for 3 hours. This treatment is sufficient to achieve complete thermodesorption of physically adsorbed water molecules from the silica surface.[12]

Preparation of $[Mo_2(MeCN)_{10}][BF_4]_4$–MCM-41 (1)

Calcined MCM-41 (0.5 g) was dehydrated and treated with a 0.012 M solution of $[Mo_2(MeCN)_{10}][BF_4]_4$ in MeCN (30 mL). The mixture was stirred at room temperature for 2 days. The solution was filtered off and the blue solid washed four times with 20 mL portions of MeCN, before drying in vacuum (10^{-2} Pa) at room temperature for several hours. Gradually, over a period of several days, the product became blue–violet. Exposure of a sample to air resulted in a colour change to grey–brown within a few minutes. Elemental analysis indicated 2.36 mass% Mo. IR (KBr, ν/cm^{-1}): 3742 w, 3455 vs, 2946 m, 2322 w, 2298 m, 2266 m, 1647 s, 1409 s, 1377 s, 1233 vs, 1084 vs, 966 s, 793 m, 743 m, 668 m, 549 w, 458 vs.

^{29}Si MAS NMR spectrum exhibited two broad resonances at $\delta = -101.9$ (Q_3) and $\delta = -110.1$ (Q_4). Deconvolution/integration gave a Q_3/Q_4 ratio of 0.26. ^{29}Si CP MAS NMR spectrum exhibited three broad resonances at $\delta = -93.7$ (Q_2), $\delta = -100.5$ (Q_3) and $\delta = -109.9$ (Q_4). ^{13}C CP MAS NMR (25 °C): δ (ppm) = 140.0 (Me**C**N, equatorial), 120 (Me**C**N, axial), 1.6, −1.5 (**Me**CN).

Preparation of $[Mo_2(\mu\text{-}O_2CMe)_2(MeCN)_6][BF_4]_2$–MCM-41 (2)

Calcined MCM-41 (0.4 g) was dehydrated and treated with a 0.014 M solution of $[Mo_2(\mu\text{-}O_2CMe)_2(MeCN)_6][BF_4]_2$ in MeCN (20 mL). The mixture was stirred at room temperature for 2 days. The solution was filtered off and the pink solid washed four times with 20 mL portions of MeCN, before drying *in vacuo* (10^{-2} Pa) at room temperature for several hours. Exposure of a sample to air resulted in an immediate (< 30 seconds) colour change to grey–brown. Elemental analysis indicated 3.62 mass% Mo. IR (KBr, ν/cm^{-1}): 3455 vs, 2984 m, 2941 m, 2894 m, 2298 w, 2266 w, 1656 s, 1531 m, 1489 m, 1444 s, 1387 s, 1232 vs, 1083 vs, 966 m, 797 m, 752 m, 673 w, 591 w, 554 w, 460 vs.

^{29}Si MAS NMR spectrum exhibited one broad resonance at $\delta = -109.8$ (Q_4). ^{29}Si CP MAS NMR spectrum exhibited three broad resonances at $\delta = -91.8$ (Q_2), $\delta = -101.2$ (Q_3) and $\delta = -109.3$ (Q_4). ^{13}C CP MAS NMR (25 °C): δ (ppm) = 186.5 (s, **O$_2$C**Me), 146.0 (Me**C**N), 129.4 (Me**C**N), 19.4 (s, O$_2$C**Me**), 4.7, 2.2, 1.0, −0.70 (**Me**CN).

Preparation of $[Mo_2(\mu\text{-}O_2CMe)_2(dppa)_2(MeCN)_2][BF_4]_2$–MCM-41 (3)

Calcined MCM-41 (0.5 g) was dehydrated and treated with a 0.011 M solution of $[Mo_2(\mu\text{-}O_2CMe)_2(dppa)_2(MeCN)_2][BF_4]_2$ in MeCN (20 mL). The mixture was stirred at room temperature for 2 days. The solution was filtered off and the pink solid washed three times with 30 mL portions of MeCN, before drying *in vacuo* (10^{-2} Pa) at room temperature for several hours. Gradually, over a period of several days, the product became pink–light brown. Exposure of a sample to air resulted in a colour change to grey within one to two hours. Elemental analysis indicated 2.21 mass% Mo. IR (KBr, ν/cm^{-1}): 3742 vw, 3457 vs, 2926 m, 2857 m, 2264 w, 1656 s, 1592 m, 1483 m, 1440 vs, 1410 s, 1236 vs, 1083 vs, 967 m, 797 s, 743 m, 697 m, 669 m, 527 m, 455 vs.

^{29}Si MAS NMR spectrum exhibited one broad resonance at $\delta = -109.6$ (Q_4). ^{29}Si CP MAS NMR spectrum exhibited two broad resonances at $\delta = -101.0$ (Q_3) and $\delta = -109.7$ (Q_4). ^{13}C CP MAS NMR (25 °C): δ (ppm) = 176.3 (s, **O$_2$C**Me), 130.2, 128.7 (dppa), 13.0 (s, O$_2$C**Me**), −1.4 (**Me**CN). ^{31}P MAS NMR spectrum (25 °C): δ (ppm) = 87.3.

Results and discussion

Synthesis and textural characterisation

The supported materials $[Mo_2(MeCN)_{10}][BF_4]_4$–MCM-41 (**1**), $[Mo_2(\mu\text{-}O_2CMe)_2(MeCN)_6][BF_4]_2$–MCM-41 (**2**) and $[Mo_2(\mu\text{-}O_2CMe)_2(dppa)_2(MeCN)_2][BF_4]_2$–MCM-41 (**3**) [dppa = bis(**d**i-**p**henyl**p**hosphine)**a**mine] were prepared by diffusion of an excess of the complex salts $[Mo_2(MeCN)_{10}][BF_4]_4$ (**1a**),[9] $[Mo_2(\mu\text{-}O_2CMe)_2(MeCN)_6][BF_4]_2$ (**2a**),[10,11] and $[Mo_2(\mu\text{-}O_2CMe)_2(dppa)_2(MeCN)_2][BF_4]_2$ (**3a**),[11] into calcined and dehydrated MCM-41 in dry acetonitrile at room temperature. The powders were washed repeatedly with acetonitrile to remove unreacted **1a** (deep blue), **2a** (red) and **3a** (red–purple).

When isolated and dried *in vacuo* at ambient temperature, **1** is light blue but the colour slowly changes to blue–violet over a period of several days to a few weeks storage under a nitrogen atmosphere at room temperature. Material **2** is initially dark pink–purple and this colour is maintained with storage under a nitrogen atmosphere. In contrast, McCann and co-workers obtained purple and brown products after reacting **1a** and **2a** respectively with silica in acetonitrile for 7–10 days.[2] Both **1** and **2** are very unstable and exposure to air results in transformation to brown–grey powders within several minutes. This parallels the behaviour of the precursor complexes **1a** and **2a** which decompose to brownish residues when exposed to air.[9,11] When isolated, **3** is pink but the colour gradually changes to pink–light brown over a period of several days to weeks storage under nitrogen at ambient temperature. At any stage the powder is sensitive and when exposed to air becomes grey within a few hours. This is in marked contrast to the precursor complex **3a** which is relatively air and moisture insensitive.

Elemental analysis indicated that **1**, **2** and **3** contained 2.36, 3.62 and 2.21 mass% Mo respectively. It follows that the surface coverage of Mo atoms in these materials is approximately in the range 2.9×10^{-25} mol nm^{-2} (0.17 Mo atoms per nm^2) to 4.7×10^{-25} mol nm^{-2} (0.28 Mo atoms per nm^2) respectively. With the molybdenum–molybdenum bond intact, the high end of this range corresponds to a surface coverage of one dimolybdenum species per 700 Å^2. The surface-fixed species are therefore isolated and well dispersed on the silica surface, a distinct advantage as far as supported catalysts are concerned. McCann *et al.* did not report loadings

or any structural characterisation for their SiO_2-fixed Mo–Mo complexes **1a** and **2a**.[2,3] It was however inferred from catalytic results that substantial structural and electronic changes had occurred upon binding the salts to the support material. The authors proposed that the surface fixation occurred at pendant silanol groups upon removal of labile MeCN ligands from the complexes.

The colours of complexes **1a–3a** get lighter when the complexes are supported on MCM-41. This moderate colour change shows that the structures of the compounds do not undergo significant changes during the fixation process, as the colours of $(Mo_2)^{4+}$-derivatives are very sensitive to changes of the ligand environment.[13] The replacement of two equatorial acetonitrile ligands by one acetamidato substituent in the case of compound **1a**, for example, changes the colour from deep blue to red–violet.[14] However, exchanges of axial ligands are of less importance for the colours of the complexes.[15] This implies that the reaction of the complexes with surface OH groups of MCM-41 either involves only the replacement of axial nitrile ligands or not more than one equatorial nitrile molecule. This would suggest a relatively weak coordination of the complexes to the MCM-41 surface (Scheme 1).

Powder XRD. The XRD pattern of the parent calcined (pristine) MCM-41 contains the characteristic and intense low angle peak at $d = 35.74$ Å which can be indexed as the d_{100} reflection on a hexagonal unit cell ($a = 2d_{100}/\sqrt{3} = 41.27$ Å, Fig. 1). The pattern also displays a broad secondary feature at about 4.6° 2θ where (110) and (200) reflections would be expected for a hexagonally ordered material such as MCM-41. The absence of resolved peaks indicates that any structural order of the material did not extend over a long range. A very similar result was obtained by Schmidt *et al.* for a purely siliceous MCM-41 prepared as in this work using the surfactant $[(C_{14}H_{29})NMe_3]Br$.[16]

The (100) reflection practically disappears on derivatisation with the complex $[Mo_2(MeCN)_{10}][BF_4]_4$ (**1a**) (Fig. 1). Identical results were obtained with the other two complexes, $[Mo_2(\mu\text{-}O_2CMe)_2(MeCN)_6][BF_4]_2$ (**2a**) and $[Mo_2(\mu\text{-}O_2CMe)_2(dppa)_2(MeCN)_2][BF_4]_2$ (**3a**). It has been shown that the intensity of the X-ray peaks in derivatised mesoporous solids decreases with decreasing 'scattering contrast' and is zero when the scattering powers of the silica wall and the pore filling material are similar.[17] This reduction in X-ray contrast might erroneously be interpreted as a severe loss of crystallinity. A qualitative indication that the pore structure in the [Mo–Mo]-derivatised materials was still intact was obtained after calcination of a sample of MCM-41 derivatised with **1a** (air: 540 °C, 24 h) resulted in restoration of the d_{100} peak to almost the same position and intensity as observed for the pristine MCM-41 ($d = 33.57$ Å, $a = 38.76$ Å, Fig. 1). The decrease in the unit cell parameter suggests a strong interaction between the mesoporous walls and the molybdenum centers. A similar observation was reported when hexane solutions of $(OiPr)_3V{=}O$ were reacted with a mesoporous, cubic MCM-48 support.[18] It was suggested that oxovanadium functional groups, multiply coordinated *via* (Si–O–V) bridges to the walls, could tend to curve the silica walls. In calcined **1**, a pore-

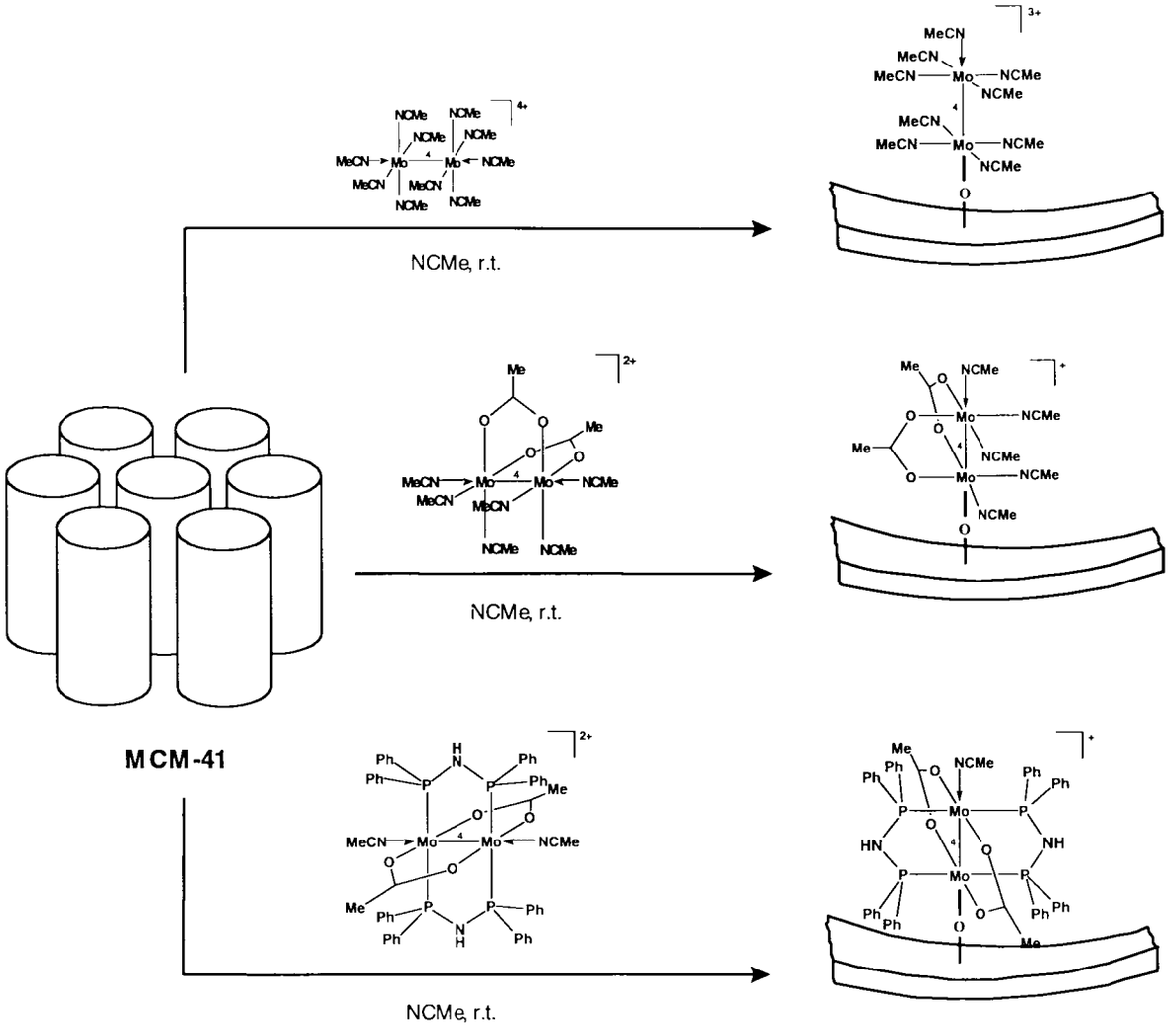

Scheme 1

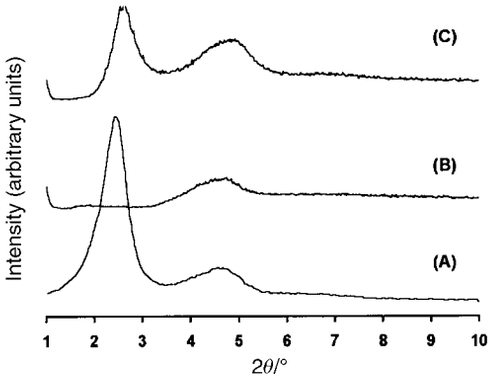

Fig. 1 Powder XRD of MCM-41: (A) as synthesised; (B) functionalised with **1a**; (C) **1** calcined at 540 °C, 24 h.

size shrinkage could be caused by the generation of isolated MoO_4 and/or polymeric oxomolybdenum species on the surface. Such species have been structurally characterised previously on the surface of calcined molybdocene-grafted MCM-41.[19] The formation of these species may also have caused a slight decrease in the long-range order of the material and therefore explain why calcination of compound **1** did not fully restore the intensity of the d_{100} reflection to that observed for pristine MCM-41.

N_2 adsorption studies. The N_2 adsorption–desorption isotherm for the pristine MCM-41 at 77 K is similar to that reported previously for MCM-41-type mesoporous solids [Fig. 2(a)]. It is defined as a reversible Type IV isotherm in the IUPAC classification,[20] and until now has only been encountered for MCM-41 materials.[16,21] At low relative pressures ($P/P_o \leqslant 0.3$) the adsorbed volume increases linearly with increasing pressure—this region corresponds to a monolayer–multilayer adsorption on the pore walls. Between $P/P_o = 0.3$ and 0.4 there is a sharp increase in the adsorbed volume, attributed to capillary condensation. At higher relative pressures multilayer adsorption takes place on the external surface, resulting in a gradual linear increase of the adsorbed volume. The BET specific surface area was calculated as 1035 $m^2\ g^{-1}$, with the cross-sectional area of a N_2 molecule taken as 16.2 $Å^2$.

Reversible Type IV isotherms similar to the pristine MCM-41 were obtained for the three functionalised solids, providing strong evidence that the mesoporous structure of the silica support was retained throughout the grafting process and that

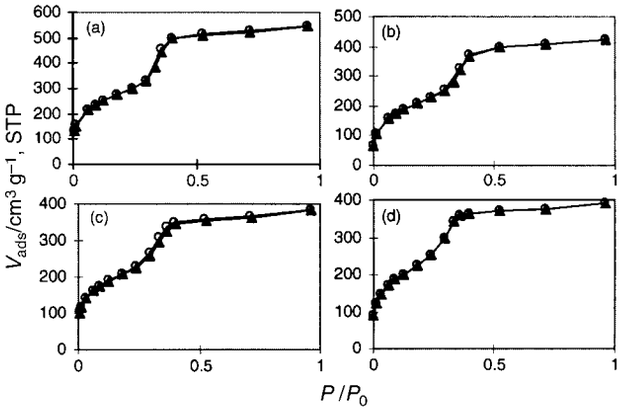

Fig. 2 N_2 adsorption–desorption isotherms recorded at 77 K of MCM-41 samples: (a) as synthesised; (b) functionalised with $[Mo_2(MeCN)_{10}][BF_4]_4$; (c) functionalised with $[Mo_2(\mu\text{-}O_2CMe)_2(MeCN)_6][BF_4]_2$; (d) functionalised with $[Mo_2(\mu\text{-}O_2CMe)_2(dppa)_2(MeCN)_2][BF_4]_2$. Triangles denote adsorption and circles correspond to desorption.

the channels remained accessible [Fig. 2(b–d)]. The BET specific surface areas were calculated as 795, 780 and 880 $m^2\ g^{-1}$ for **1**, **2** and **3** respectively. The main difference between these isotherms and that of the starting material is in the limiting uptake at high P/P_o. For example, the total volumes of adsorbed N_2 at 77 K and $P/P_o = 0.6$ are 0.74, 0.57, 0.51 and 0.53 $cm^3\ g^{-1}$ for parent calcined MCM-41, **1**, **2** and **3** respectively. This approximate 30% decrease in the total volume of adsorbed N_2 can be attributed to successful grafting of the molybdenum complex fragments on the internal surfaces of the silica support.

To investigate how the dimolybdenum complexes react and bind with the mesoporous silica, we have studied the materials using solid-state MAS NMR (^{13}C, ^{29}Si, ^{31}P) and FTIR spectroscopy.

Solid-state NMR and FTIR spectroscopy

Fig. 3 shows the ^{29}Si MAS and CP MAS NMR spectra of pristine MCM-41 and $[Mo_2(MeCN)_{10}][BF_4]_4$–MCM-41 (**1**). The ^{29}Si MAS spectrum of the starting material exhibits two broad overlapping peaks at $\delta = -101.3$ and -109.8 assigned to, respectively, Q_3 and Q_4 units of the silica framework [$Q_3/Q_4 = 1.0$, $Q_n = Si(OSi)_n(OH)_{4-n}$]. Even given the *ca.* 8% error inherent in spectral deconvolution, the Q_3/Q_4 population ratio reflects the extent of silanol condensation, indicating the large number of OH groups present at the surface.[22] A small amount of Q_2, as a faint peak at approximately $\delta = -92$, is also present. The ^{29}Si CP MAS NMR spectrum shows a marked increase in the relative intensity of the Q_2 and Q_3 lines in comparison with the ^{29}Si MAS spectrum, confirming that these silicons are attached to hydroxy groups. The successful anchoring of the complex **1a** at the channel surface is demonstrated by Fig. 3(B). Both ^{29}Si MAS ($Q_3/Q_4 = 0.26$) and CP MAS NMR spectra clearly show the diminished relative intensity of the Q_2 and Q_3 peaks, indicating the esterification of the free hydroxy groups by substitution of the MeCN ligands in the complexes. A decrease in the population of isolated OH groups was further confirmed qualitatively by a decrease in the relative intensity of the sharp IR absorption band at 3742 cm^{-1} associated with free OH groups on the silica surface (Fig. 4).[23] In the OH stretching region a very broad

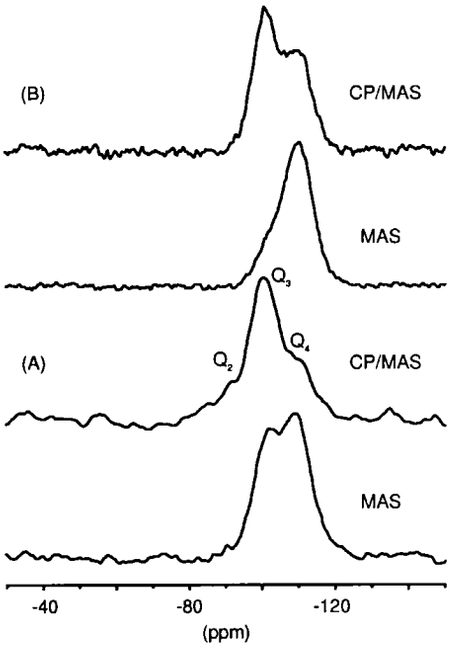

Fig. 3 ^{29}Si CP MAS and MAS NMR of MCM-41 at room temperature: (A) as synthesised; (B) functionalised with $[Mo_2(MeCN)_{10}][BF_4]_4$.

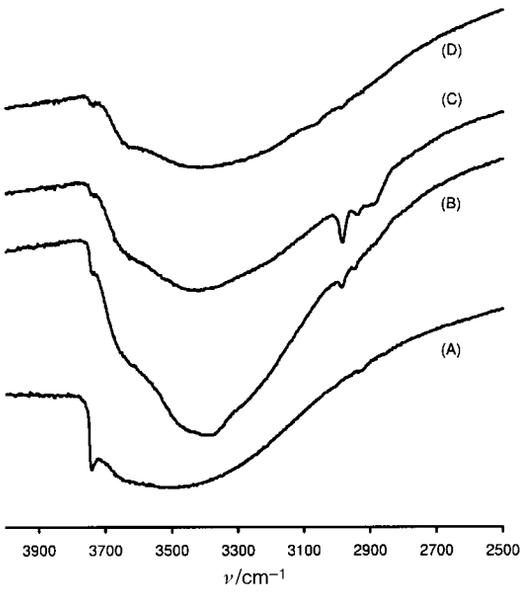

Fig. 4 FTIR spectra in the range 4000–2500 cm^{-1} of the samples: (A) pure calcined MCM-41 (dehydrated at 160 °C *in vacuo* for 3 h); (B) MCM-41 functionalised with $[Mo_2(MeCN)_{10}][BF_4]_4$; (C) MCM-41 functionalised with $[Mo_2(\mu\text{-}O_2CMe)_2(MeCN)_6][BF_4]_2$; (D) MCM-41 functionalised with $[Mo_2(\mu\text{-}O_2CMe)_2(dppa)_2(MeCN)_2][BF_4]_2$.

absorption band is also observed at *ca.* 3600 cm^{-1}, assigned to water and/or hydrogen-bonded SiOH groups. Similar results were obtained for **2** and **3**.

The ^{29}Si CP MAS NMR spectrum of **1** shows that there are still a large number of unreacted Q_3 silicon atoms in the composite material. Similar results were obtained with ferrocenyl-modified MCM-41 and MCM-48, prepared *via* ring-opening reaction of the strained [1]ferrocenophane $[Fe\{(\eta\text{-}C_5H_4)_2SiMe_2\}]$.[24] These silanol groups may be contained within the wall framework and sequestered from electrophilic attack. In addition, there may be a large number of hydrogen bonded Q_3 silanols present at the surface, $(SiO)_3Si—OH–OH—Si(SiO)_3$, which are unreactive to the dimolybdenum complexes. These types of silanols have previously been shown to be inert to silylating agents, for example.[23] In a detailed study of the surface chemistry of MCM-41, Zhao *et al.* determined the number of silanol groups per nm^2 to be 2.5 for a material which was prepared and treated in a similar way to ours (as-synthesised sample calcined at 540 °C for 24 h in air, then dried at 110 °C for 24 h *in vacuo*).[23] Our sample was calcined at the same temperature for 6 h in air, then dehydrated and outgassed at 160 °C for 3 h *in vacuo* prior to solvent impregnation of the complexes **1a–3a**. Zhao *et al.* estimated that 0.7 of the silanol groups were isolated single hydroxy groups and the remainder were hydrogen bonded silanols with a small contribution from geminal silanols. Furthermore, an FTIR study showed that outgassing temperatures of 200 °C or higher were required before dehydroxylation of hydrogen-bonded and geminal SiOH groups took place to a significant extent, to form siloxane bonds and simultaneously more free SiOH groups. Dehydroxylation of single SiOH groups is impossible since they are too far apart (0.5 nm) and such a process would necessarily involve the unfavourable formation of highly strained linked structures.

In our derivatised materials, the surface coverage of Mo atoms is in the range 0.15 to 0.3 nm^{-2}, somewhat lower than the above value for the concentration of free hydroxy groups on the surface of pristine MCM-41. The low loading could be due to steric crowding of the guest complexes which may prevent reaction with a large fraction of surface silanol sites. In general it has been estimated that 8–27% of the silicon atoms in MCM-41 have pendant OH groups and that the average separation of these groups is in the range 5 to 10 Å. It seems unlikely therefore that the dimolybdenum complexes could undergo bipodal anchoring to the silica surface, as suggested by McCann *et al.* for silica-fixed **1a** and **2a**.[1–3] Monopodal anchoring, as depicted in Scheme 1, seems more plausible as the dominant mechanism for surface attachment. A similar conclusion was reached for MCM-41 and MCM-48 modified with the *ansa*-bridged titanocene $[SiMe_2\{(\eta^5\text{-}C_5H_4)_2\}]TiCl_2$.[25] However, it is worth noting that tripodal anchoring of organometallic fragments to the surface of MCM-41 has been reported, for example with Cp_2TiCl_2-grafted MCM-41.[26]

The ^{13}C CP MAS NMR spectrum of $[Mo_2(MeCN)_{10}][BF_4]_4$–MCM-41 (**1**) exhibits two broad peaks at δ *ca.* 140 and 120 attributed to Me**C**N and two peaks at $\delta = 1.6$ and -1.5 attributed to equatorial and axial **Me**CN, respectively [Fig. 5(B)]. Material **1** is very air and moisture sensitive and on several occasions our sample began to decompose during packing of the NMR rotor and spectrum acquisition resulting in many broad peaks in the region $\delta = 3.0$ to 0.5. Compared to the ^{13}C CP MAS NMR spectrum of the complex $[Mo_2(MeCN)_{10}][BF_4]_4$ (**1a**), these peaks are shifted further upfield. The isotropic chemical shifts of **1a** are at $\delta = 149.5$ and 148.0 (Me**C**N, equatorial), around $\delta = 123.6$ (Me**C**N, axial), and $\delta = 3.5$ and 0.8 attributed to the equatorial and axial **Me**CN, respectively [Fig. 5(A)]. The IR spectrum of **1** contains in the nitrile region three stretches at 2322, 2298 and 2266 cm^{-1} [Fig. 6(A), Table 1]. These are shifted to significantly lower wavenumbers compared to the corresponding bands for **1a** (2359, 2322, 2293 cm^{-1}), indicating a weakening of the bond.

The room-temperature solid state ^{13}C CP MAS NMR spectrum of $[Mo_2(\mu\text{-}O_2CMe)_2(MeCN)_6][BF_4]_2$–MCM-41 (**2**) is shown in Fig. 7. Five broad resonances are observed at δ *ca.* 186, 146, 129, 19 and 2 attributed to **C–O**, Me**C**N, O_2C**Me** and **Me**CN, respectively. All these signals are broader than those of the related crystalline compound $[Mo_2(\mu\text{-}O_2CMe)_2(MeCN)_6][BF_4]_2$ (**2a**). The broadness is due to the range of

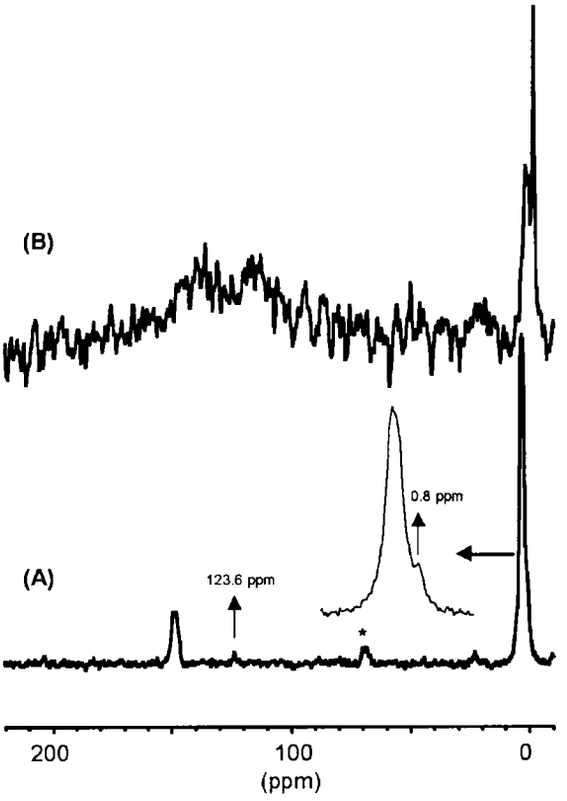

Fig. 5 ^{13}C CP MAS NMR at room temperature: (A) $[Mo_2(MeCN)_{10}][BF_4]_4$, 1450 transients; (B) $[Mo_2(MeCN)_{10}][BF_4]_4$–MCM-41, 22 352 transients. * denotes spinning sidebands.

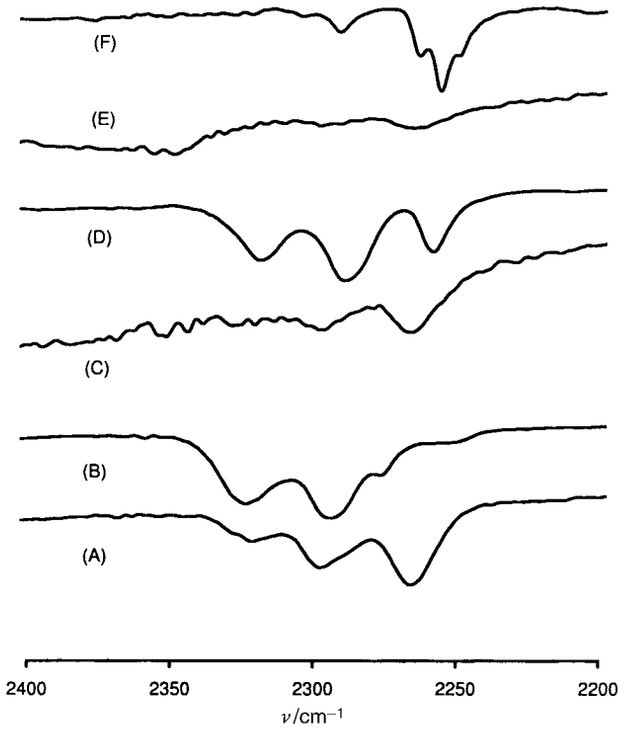

Fig. 6 FTIR spectra in the range 2400–2200 cm^{-1} of the samples: (A) MCM-41 functionalised with **1a**; (B) $[Mo_2(MeCN)_{10}][BF_4]_4$ (**1a**); (C) MCM-41 functionalised with **2a** (D); $[Mo_2(\mu\text{-}O_2CMe)_2(MeCN)_6][BF_4]_2$ (**2a**); (E) MCM-41 functionalised with **3a**; (F) $[Mo_2(\mu\text{-}O_2CMe)_2(dppa)_2(MeCN)_2][BF_4]_2$ (**3a**).

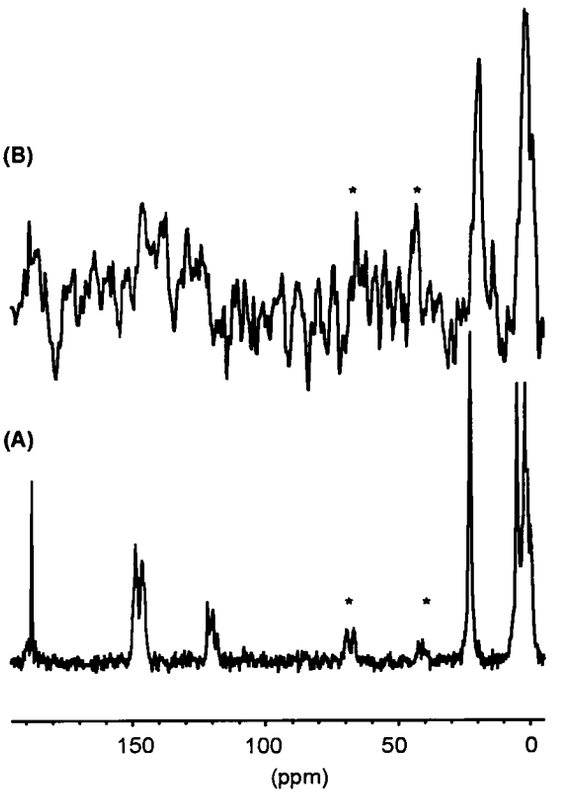

Fig. 7 ^{13}C CP MAS NMR at room temperature: (A) $[Mo_2(\mu\text{-}O_2CMe)_2(MeCN)_6][BF_4]_2$, 14 889 transients; (B) $[Mo_2(\mu\text{-}O_2CMe)_2(MeCN)_6][BF_4]_2$–MCM-41, 16 680 transients. * denotes spinning sidebands.

chemically different environments in which the molecule is located. A large number of scans were required to obtain these spectra. In the ^{13}C CP MAS NMR spectrum of the complex **2a** five peaks are observed at $\delta = 187.6$, 148 (doublet), 121 (doublet), 22.7 and 2.1 (multiplet) attributed to **C–O**, Me**C**N (equatorial and axial), O_2C**Me** and **Me**CN (equatorial and axial), respectively. The IR spectrum of the solid **2** (KBr matrix) contains the carboxylate ν_{asym} (OCO) and ν_{sym} (OCO) vibrations at 1489 and 1440 cm^{-1}, respectively (Table 1). The presence of the bridging acetates is a clear indication that the molybdenum–molybdenum bond is intact. Weak bands attributable to the MeCN ligands are present at 2298 and 2266 cm^{-1}. Complex **2a** exhibits two nitrile vibrations in similar positions (2288, 2259 cm^{-1}) and a third one at 2319 cm^{-1}, not observed in the spectrum of **2**.

For the material $[Mo_2(\mu\text{-}O_2CMe)_2(dppa)_2(MeCN)_2][BF_4]_2$–MCM-41 (**3**) the bridging acetato complex is clearly identified by ν_{asym} (OCO) at 1483 cm^{-1} and the very strong ν_{sym} (OCO) at 1440 cm^{-1} in the IR spectrum (Table 1). The C–C and C–H vibrations attributed to the dppa ligand are very similar to the initial complex. Only one nitrile vibration was observed in the IR spectrum, at 2264 cm^{-1}. Complex **3a** has one main band in this region (2255 cm^{-1}). The ^{31}P MAS spectrum of **3** (not shown) exhibits a broad singlet for the coordinated dppa ligand at $\delta = 87.3$, shifted downfield slightly from that observed for the free complex $[Mo_2(\mu\text{-}O_2CMe)_2(dppa)_2(MeCN)_2][BF_4]_2$ ($\delta = 82.6$, free dppa exhibits a chemical shift of $\delta = 42.0$ ppm[27]). The difference between these shifts is small and this suggests that the interaction between the complex **3a** and MCM-41 has only a minor effect on the shielding of the phosphorus nuclei. It may be inferred therefore that binding of the complex to the silica surface occurs by substitution of a surface silanol group for an axial acetonitrile molecule in the complex, as depicted in Scheme 1. It is known that in complexes of the type $Mo_2(\mu\text{-}O_2CMe)_2(dppa)_2X_2$ (X = Cl, Br, I) the nature of the axially coordinated halo ligands has little influence on the ^{31}P MAS chemical shifts (the Mo–X distances are comparatively long, indicating only weak Mo–halo interactions).[27] Similarly, in complex **3a**, a long axial Mo–N distance indicates that the acetonitrile molecules might very easily be replaced by stronger donors. ^{31}P MAS NMR studies of **3** also suggested that one phosphorus-containing by-product is formed ($\delta = 29.3$) which we attribute to a decomposition product (*e.g.* phosphine oxide).

The ^{13}C CP MAS NMR spectrum of **3** exhibits a weak broad peak at 176.2 (**C–O**), two sharp resonances at 130.9 and 128.7 (phenyl groups) and two well-defined singlets at 13.0 (**Me**CO_2) and −1.4 (**Me**CN) (Fig. 8).

Table 1 Selected IR data for the complexes **1a–3a** and corresponding MCM-41-supported derivatives (KBr discs, ν_{max} in cm^{-1})

	ν(C≡N)	$\nu_{asym}(CO_2)$	$\nu_{sym}(CO_2)$
$[Mo_2(MeCN)_{10}][BF_4]_4$ **1a**	2359, 2322, 2293, 2276sh, 2253	—	—
$[Mo_2(MeCN)_{10}][BF_4]_4$–MCM-41 **1**	2322, 2298, 2266	—	—
$[Mo_2(\mu\text{-}O_2CMe)_2(MeCN)_6][BF_4]_2$ **2a**	2288, 2259, 2319	1501	1444
$[Mo_2(\mu\text{-}O_2CMe)_2(MeCN)_6][BF_4]_2$–MCM-41 **2**	2298, 2266	1489	1440
$[Mo_2(\mu\text{-}O_2CMe)_2(dppa)_2(MeCN)_2][BF_4]_2$ **3a**	2291, 2262sh, 2255, 2249sh	1482	1436
$[Mo_2(\mu\text{-}O_2CMe)_2(dppa)_2(MeCN)_2][BF_4]_2$–MCM-41 **3**	2264	1483	1440

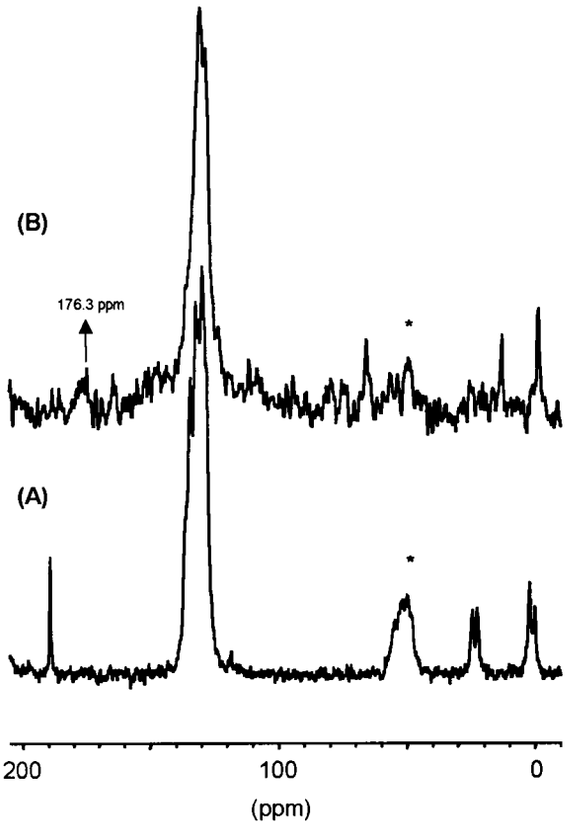

Fig. 8 ^{13}C CP MAS NMR at room temperature: (A) $[Mo_2(\mu\text{-}O_2CMe)_2(dppa)_2(MeCN)_2][BF_4]_2$, 1055 transients; (B) $[Mo_2(\mu\text{-}O_2CMe)_2(dppa)_2(MeCN)_2][BF_4]_2$–MCM-41, 21 174 transients. * denotes spinning sidebands.

Conclusions

The quadruply bonded dimolybdenum complex salts $[Mo_2(MeCN)_{10}][BF_4]_4$, $[Mo_2(\mu\text{-}O_2CMe)_2(MeCN)_6][BF_4]_2$ and $[Mo_2(\mu\text{-}O_2CMe)_2(dppa)_2(MeCN)_2][BF_4]_2$ react with purely siliceous MCM-41 in acetonitrile to give unstable composite materials in which solvent-stabilised cationic molybdenum fragments are isolated and well dispersed on the silica surface. Powder XRD and N_2 adsorption studies confirm that the textural properties of the high surface area mesoporous host are retained throughout the grafting process. Solid-state MAS NMR and IR spectroscopy indicate that the mechanism of surface attachment involves the displacement of labile acetonitrile ligands, most likely in the axially coordinated position, from the complexes by reaction with isolated nucleophilic silanol groups at the silica surface. In can be inferred from the spectral data that the molybdenum–molybdenum bond is intact in all the functionalised solids and that the complexes undergo only a weak interaction with the surface. Investigations are ongoing to further probe the structure of the supported molybdenum species and to test the materials as catalysts for catalytic polymerisation reactions.

Acknowledgements

We thank PRAXIS XXI and FEDER for partial funding. P.F. (BD) thanks PRAXIS XXI for a grant. I.S.G. is grateful to the CRUP (Acções Integradas Programme) for generous support. W.M.X. is grateful to the Alexander von Humboldt-foundation and G.Z. to the Katholischer Akademischer Ausländerdienst for a grant.

References

1 M. McCann, in *Catalysis by Di- and Polynuclear Metal Cluster Complexes*, ed. R. D. Adams and F. A. Cotton, Wiley-VCH, New York, 1998, pp. 145–166
2 M. McCann, E. M. G. Coda and K. Maddock, *J. Chem. Soc., Dalton Trans.*, 1994, 1489.
3 M. McCann and E. M. G. Coda, *J. Mol. Catal. A: Chem.*, 1996, **109**, 99.
4 F. E. Kühn, J. R. Ismeier, D. Schön, W. M. Xue, G. Zhang and O. Nuyken, *Macromol. Rapid Commun.*, in press.
5 J. Smith, W. Mowat, D. A. Whan and E. A. V. Ebsworth, *J. Chem. Soc., Dalton Trans.*, 1974, 1742; Q. Zhuang, A. Fukuoka, T. Fujimoto, K. Tanaka and M. Ichikawa, *J. Chem. Soc., Chem. Commun.*, 1991, 745.
6 Y. Iwasawa, S. Ogasawara, Y. Sato and H. Kuroda, *Chem. Uses Molybdenum, Proc. Int. Conf. 4th*, 1982, 283.
7 K. Moller and T. Bein, *Chem. Mater.*, 1998, **10**, 2950; T. Maschmeyer, *Curr. Opin. Solid State Mater. Sci.*, 1998, **3**, 71; R. A. Sheldon, I. W. C. E. Arends and H. E. B. Lempers, *Catal. Today*, 1998, **41**, 387.
8 C. T. Kresge, M. E. Leonowicz, W. J. Roth, J. C. Vartuli and J. S. Beck, *Nature*, 1992, **359**, 710; J. S. Beck, J. C. Vartuli, W. J. Roth, M. E. Leonowicz, C. T. Kresge, K. D. Schmitt, C. T.-W. Chu, D. H. Olson, E. W. Sheppard, S. B. McCullen, J. B. Higgins and J. L. Schlenker, *J. Am. Chem. Soc.*, 1992, **114**, 10834.
9 F. A. Cotton and K. J. Wiesinger, *Inorg. Chem.*, 1991, **30**, 871.
10 F. A. Cotton, A. H. Reid and W. Schwotzer, *Inorg. Chem.*, 1985, **24**, 3965; G. Pimblett, C. D. Garner and W. Clegg, *J. Chem. Soc., Dalton Trans.*, 1986, 1257.
11 F. A. Cotton and F. E. Kühn, *Inorg. Chim. Acta*, 1996, **252**, 257.
12 C. P. Jaroniec, R. K. Gilpin and M. Jaroniec, *J. Phys. Chem. B*, 1997, **101**, 6861; C. P. Jaroniec, M. Kruk, M. Jaroniec and A. Sayari, *J. Phys. Chem. B*, 1998, **102**, 5503.
13 F. A. Cotton and R. A. Walton, *Multiple Bonds between Metal Atoms*, Oxford University Press, New York, 1993.
14 F. A. Cotton, L. Daniels, S. C. Haefner and F. E. Kühn, *Inorg. Chim. Acta*, 1999, **287**, 159.
15 W. M. Xue, F. E. Kühn, G. Zhang, E. Herdtweck and G. Raudaschl-Sieber, *J. Chem. Soc., Dalton Trans.*, 1999, 4103.
16 R. Schmidt, M. Stöcker, E. Hansen, D. Akporiaye and O. H. Ellestad, *Microporous Mater.*, 1995, **3**, 443.
17 B. Marler, U. Oberhagemann, S. Voltmann and H. Gies, *Microporous Mater.*, 1996, **6**, 375.
18 M. Morey, A. Davidson, H. Eckert and G. D. Stucky, *Chem. Mater.*, 1996, **8**, 486.
19 I. J. Shannon, T. Maschmeyer, R. D. Oldroyd, G. Sankar, J. M. Thomas, H. Pernot, J.-P. Balikdjian and M. Che, *J. Chem. Soc., Faraday Trans.*, 1998, **94**, 1495.
20 S. Brunauer, L. S. Deming, W. S. Deming and E. Teller, *J. Am. Chem. Soc.*, 1940, **62**, 1723.
21 O. Franke, G. Schulz-Ekloff, J. Rathousky, J. Starek and A. Zunkal, *J. Chem. Soc., Chem. Commun.*, 1993, 724; P. J. Branton, P. G. Hall and K. S. W. Sing, *J. Chem. Soc., Chem. Commun.*, 1993, 1257.
22 A. A. Romero, M. D. Alba, W. Zhou and J. Klinowski, *J. Phys. Chem. B*, 1997, **101**, 5294.
23 X. S. Zhao, G. Q. Lu, A. K. Whittaker, G. J. Miller and H. Y. Zhu, *J. Phys. Chem. B*, 1997, **101**, 6525.
24 S. O'Brien, J. M. Keates, S. Barlow, M. J. Drewit, B. R. Payne and D. O'Hare, *Chem. Mater.*, 1998, **10**, 4088; P. Ferreira, I. S. Gonçalves, F. Mosselmans, M. Pillinger, J. Rocha and A. Thursfield, *Eur. J. Inorg. Chem.*, 2000, 97.
25 P. Ferreira, I. S. Gonçalves, F. E. Kühn, M. Pillinger, J. Rocha, A. M. Santos and A. Thursfield, *Eur. J. Inorg. Chem.*, 2000, 551.
26 T. Maschmeyer, F. Rey, G. Sankar and J. M. Thomas, *Nature*, 1995, **378**, 159; L. Marchese, E. Gianotti, V. Dellarocca, T. Maschmeyer, F. Rey, S. Coluccia and J. M. Thomas, *Phys. Chem. Chem. Phys.*, 1999, **1**, 585.
27 D. L. Arnold, F. A. Cotton and F. E. Kühn, *Inorg. Chem.*, 1996, **35**, 4733.